CHAPTER IV

RESULTS AND DISCUSSION

4.1 Fixation of Octadecyl Silyl Group

Silica Hi-Sil®233 was treated with octadecyltrichlorosilane (ODS) to provide the bonded monolayer. The changes in the IR adsorption spectra following the treatment with ODS are listed in Table 4.1. The adsorption at 2855 and 2925 cm^{-1} due to the alkyl groups attributable to the ODS group appeared. The spectrum at 1000-1100 cm^{-1} due to the stretching vibration of Si-O were enlarged slightly, whereas the broad band at 3300-3600 cm^{-1} due to the OH group of silica were decreased. These spectra qualitatively indicate that the ODS group was fixed on the silica surface.

Table 4.1. Changes of IR spectra of silica by the treatment with ODS

Functional groups	Band cm^{-1}	SiO_2 Absorbance	ODS SiO_2 Absorbance
$\nu(CH_3)$	2855, 2925	0, 0	0.2450, 0.3472
ν(Si-O)	1000-1100	2.6787	2.7651
ν(Si-OH)	3300-3600	0.3651	0.3604
$\delta(CH_3)$	1463	0	0.1846

The TG-DTA results are listed in Table 4.2. The weight loss due to the ODS group is calculated by subtracting the weight loss of adsorbed water from total weight loss of ODS silica in the range of 170-800 °C (Ogawa et al., 1994). The silica ODS/0.3 indicates the silica reacted with ODS 0.3 ml.

DTA analysis indicates that the decomposition of the ODS group on the silica surface starts at 170 °C, and is maximized at about 259 °C.

Table 4.2 Decreased weight based on the TG curves

Silica	170-800 °C	ODS (wt %)
	Adsorbed water + ODS (wt %)	
Untreated	0.8	0
ODS silica/0.3	4.0	3.2
ODS silica/0.5	5.4	4.6
ODS silica/0.7	6.3	5.5
ODS silica/1.0	7.9	7.1
ODS silica/1.5	10.1	9.3
ODS silica/2.0	11.2	10.4
ODS silica/3.5	11.6	10.8

4.2 Adsorption of CTAB and Bonded ODS on Silica Hi-Sil®233

The CTAB adsorption isotherm and the amount of bonded ODS on Silica Hi-Sil®233 are shown in Figure 4.1. The CTAB adsorption isotherm can be divided into two of the characteristic regions (region II and IV). In region II, 1800-3000 μM, the very steep slope indicates CTAB aggregation on the silica surface. The plateau region shows the maximum adsorption of CTAB on silica of approximately 300 μmoles/g and the critical micelle concentration (CMC) of roughly 3000 μM. For the chemically bonded ODS on silica, no clear regions are noticeable. The maximum adsorption of bonded monolayer of

ODS on silica surface is 340 μmoles/g. That the maximum CTAB adsorption is less may be the effect of electrostatic repulsion between the CTAB headgroups.

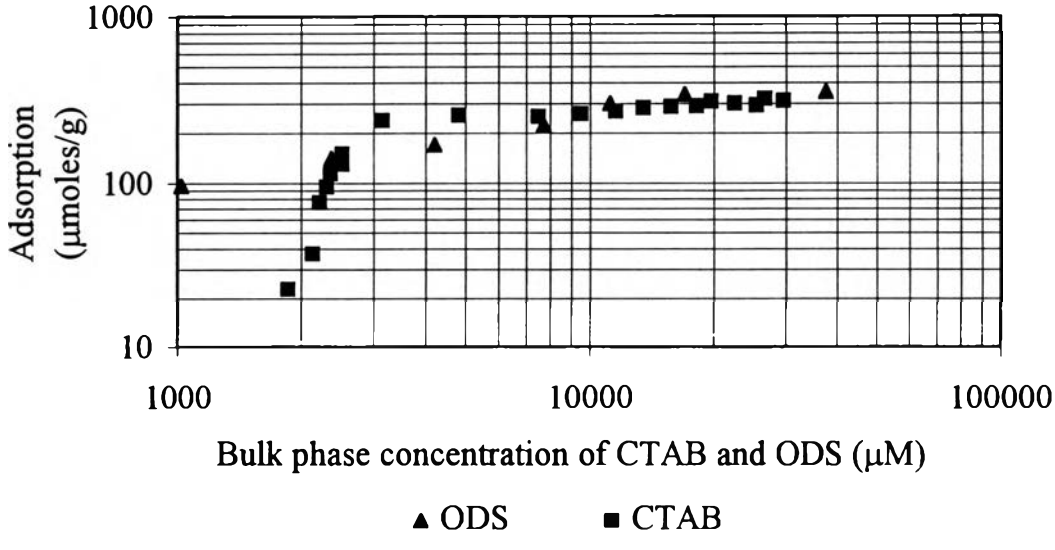

Figure 4.1 CTAB and bonded ODS adsorption isotherm on Hi-Sil®233.

It has previously been reported that the presence of a high concentration of alcohol increased the adsorption of surfactant onto alumina (Yeskie, 1988). As can be seen in Figure 4.2, CTAB adsorption is changed only very slightly by the presence of phenol at 2097 μM. The adsorption of CTAB onto silica is also not affected by low concentrations of TCE. Consequently, it was assumed that the surfactant adsorption is independent of the low organic solute concentrations used in these experiments.

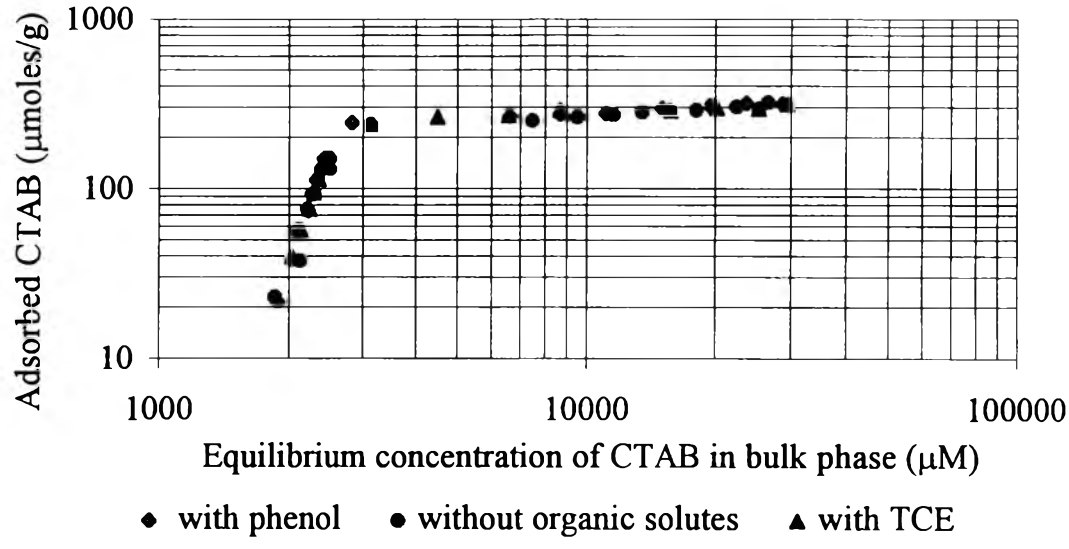

Figure 4.2 Effect of phenol and TCE on CTAB adsorption.

4.3 Adsolubilization of Phenol and TCE

The relation between the amount of adsolubilized phenol and adsorption of CTAB and ODS is presented in Figure 4.3. The decrease in phenol adsolubilization above about 250 moles of adsorbed CTAB/g of solid is caused by CTAB micelles in the bulk phase. For chemically bonded ODS on silica, the amount of adsolubilized phenol increases over the entire range of bonded ODS concentration.

Figure 4.4 shows the relation between the equilibrium concentration of phenol and the equilibrium concentration of CTAB and ODS in bulk phase. The concentration of phenol in aqueous phase decreases with increasing CTAB concentration in aqueous phase. When the concentration of CTAB on centration in bulk phase is higher than 3000 μM, the phenol concentration in

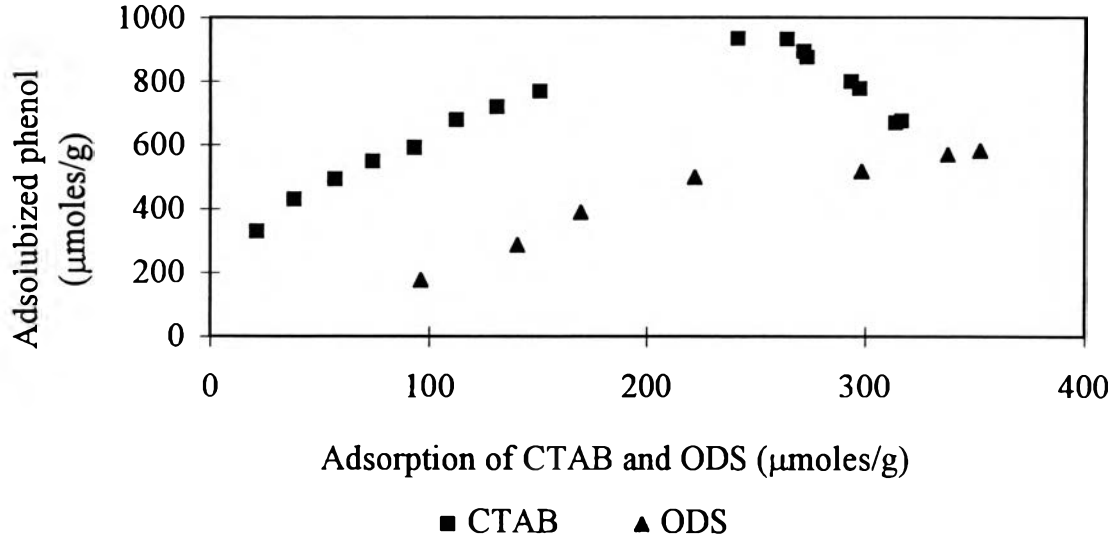

Figure 4.3 Effect of adsorption of CTAB and ODS on adsolubilized phenol.

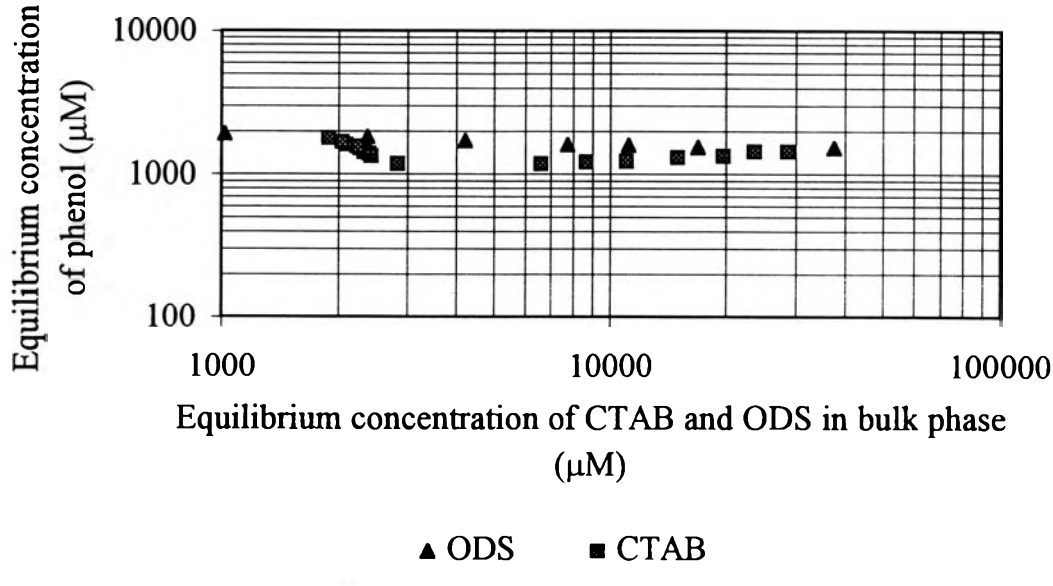

Figure 4.4 Relation between equilibrium concentration of phenol and equilibrium concentration of CTAB and ODS in bulk phase.

aqueous phase increases with the occurrence of micelles that are solubilized by phenol. This effect is also shown in Figure 4.3 indicating the decrease of adsolubilized phenol with increasing CTAB adsorption on silica. The adsolubilized phenol into bonded ODS decreases in the first range and reaches nearly constant value above the 3000 μM of ODS bulk phase concentration.

In the adsolubilization studies, adsolubilization is usually quantified using the partition coefficient, P_a, and the adsolubilization constant, K_s. P_a is defined as the ratio of solute concentration in the admicelles (defined as moles adsolubilized solute per unit total volume) to that in aqueous phase:

$$P_a = [C^*]/[C]$$

where [C*] and [C] are concentrations based on the total solution volume. K_s is defined as

$$K_s = [C^*]/\{[S][C]\} = P_a/[S]$$

where [S] is the adsorbed surfactant concentration (M). In a plot of P_a versus [S], the slope gives the value of K_s (M^{-1}), if K_s remains constant.

The partition coefficient (P_a) of phenol increases linearly with CTAB adsorption below 250 μmoles/g in the absence of micelles(see Figure 4.5) For the bonded ODS, it shows a same trend as the P_a in CTAB admicelles. Furthermore, the figure also shows the higher P_a of phenol in CTAB admicelles than that in bonded ODS at all adsorption.

In Figure 4.6, a monotonic decrease at very low CTAB adsorption level is observed. It possibly due to the blocking of some very small pores in

the silica particles by the second layer of CTAB. In the part of bonded ODS, the adsolubilization constants of phenol present nearly the constant values at all adsorption of ODS.

The adsolubilization of TCE is showed in Figure 4.7-4.10. These figures indicate the same trends as the adsolubilization of phenol. Figure 4.7 shows the adsolubilizations of TCE into both of CTAB admicelles and bonded monolayer of ODS on silica surface with nearly the same values with the adsorption below 250 μmoles/g. Figure 4.8 shows the relation between equilibrium concentration of TCE and equilibrium concentration of CTAB and ODS in bulk phase. This figure indicates the effect of micelles on increasing of TCE concentration in bulk phase and this also decreases the amount of adsolubilized TCE into CTAB admicelles (see Figure 4.7).

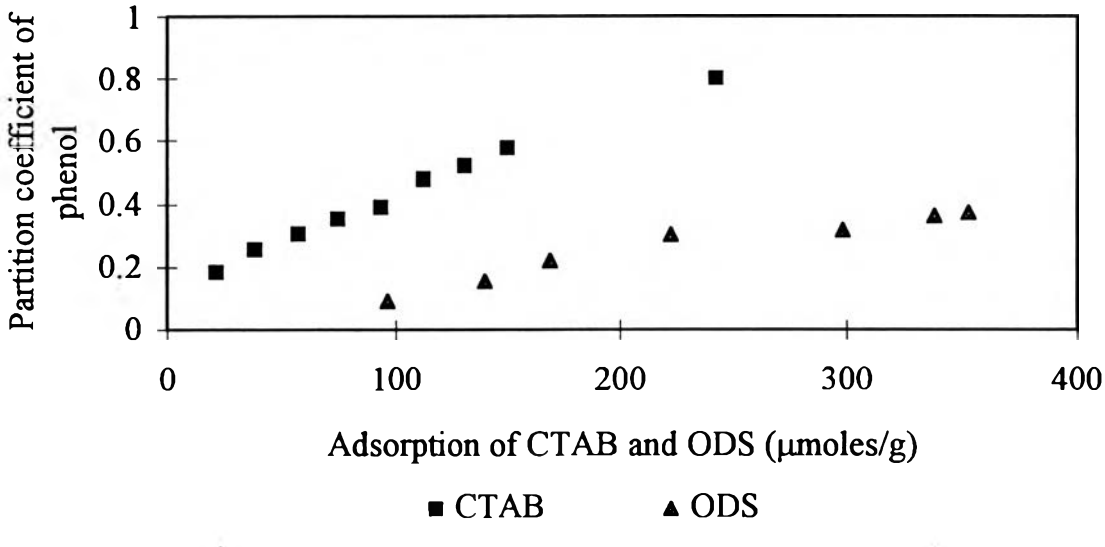

Figure 4.5 Effect of adsorption of CTAB and ODS on partition coefficient of phenol.

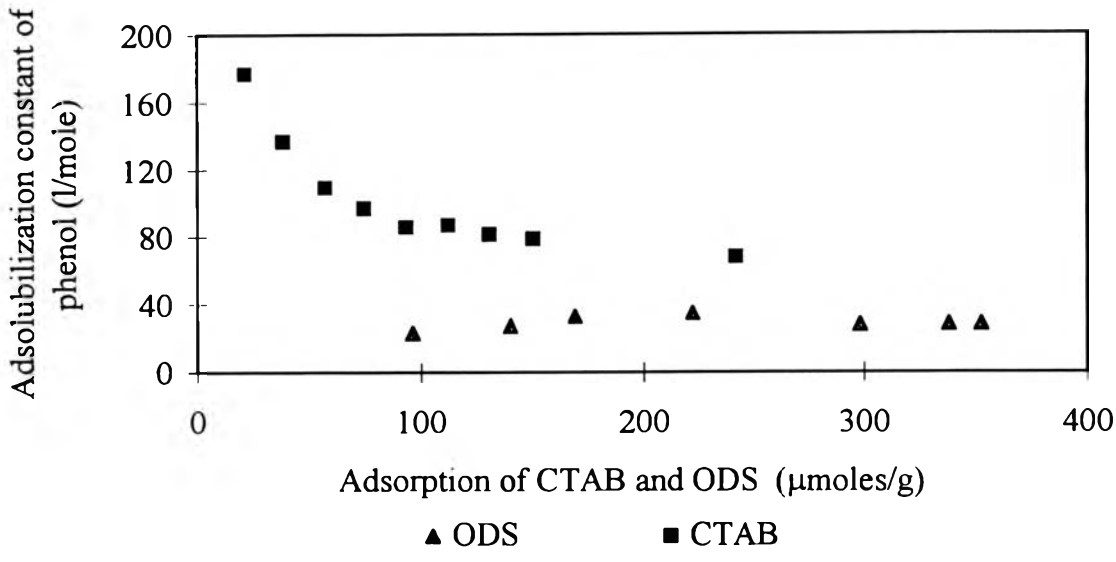

Figure 4.6 Effect of adsorption of CTAB and ODS on adsolubilization constant of phenol.

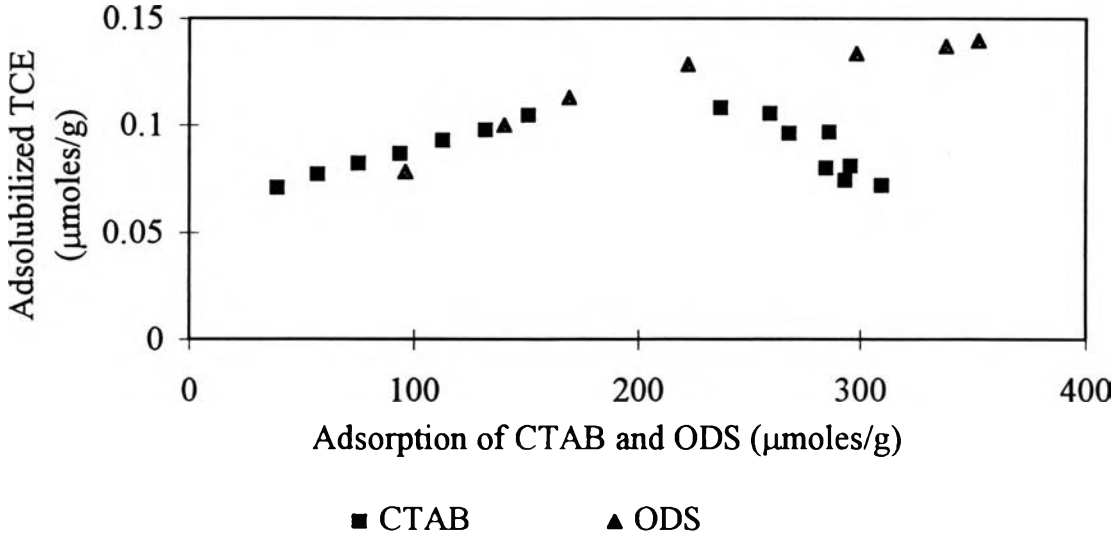

Figure 4.7 Effect of adsorption of CTAB and ODS on adsolubilized TCE.

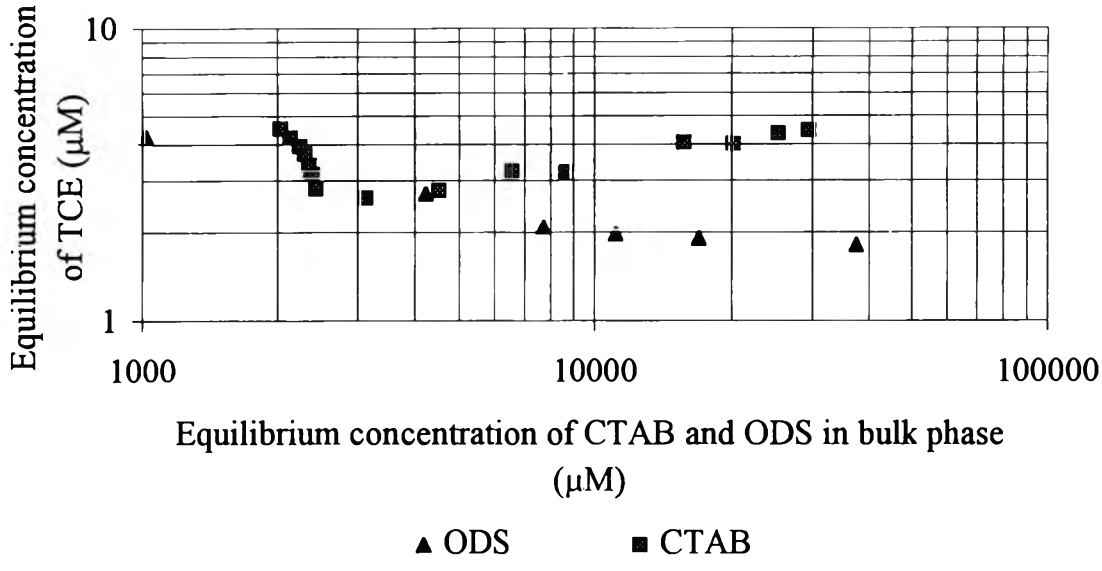

Figure 4.8 Relation between equilibrium concentration of TCE and equilibrium concentration of CTAB and ODS in bulk phase.

Figure 4.9 presents the effect of CTAB and ODS adsorption on partition coefficient of TCE. The figure shows that the partition coefficient of TCE in CTAB admicelles is very little higher than that in bonded ODS. These results may be the nonpolar property of TCE that tends to partition into the hydrophobic core of admicelles, and the bonded monolayer has only the core region. The adsolubilization constant of phenol give the different values for CTAB admicelles and bonded monolayer of ODS. This is because of a strong tendency of polar molecule of phenol in adsolubilizing into the palisade layer. The bonded ODS monolayer does not have the palisade layer, thus the adsolubilization constant of phenol is lower than that of admicelles.

Figure 4.10 indicates the relation between the adsolubilization constant of TCE and CTAB and ODS adsorption. The monotonic reduction of adsolubilization constants is observed at low CTAB adsorption level that can be explained by the same reason as Figure 4.6. For bonded ODS, the adsolubilization constant increases with increasing the adsorption of bonded ODS and becomes constant at complete adsorption. These are possibly due to the increase in hydrocarbon layer on silica in the first range causing the increase amount of adsolubilized TCE. Above 250 μmoles/g, the tighter packing of bonded ODS molecules may be the result in decreasing TCE adsolubilization constant.

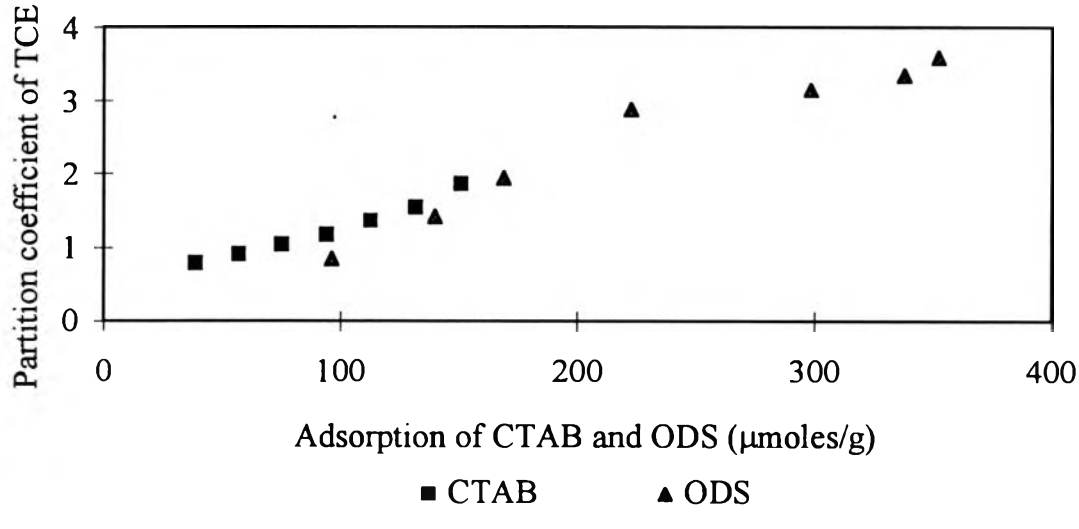

Figure 4.9 Effect of adsorption of CTAB and ODS on partition coefficient of TCE.

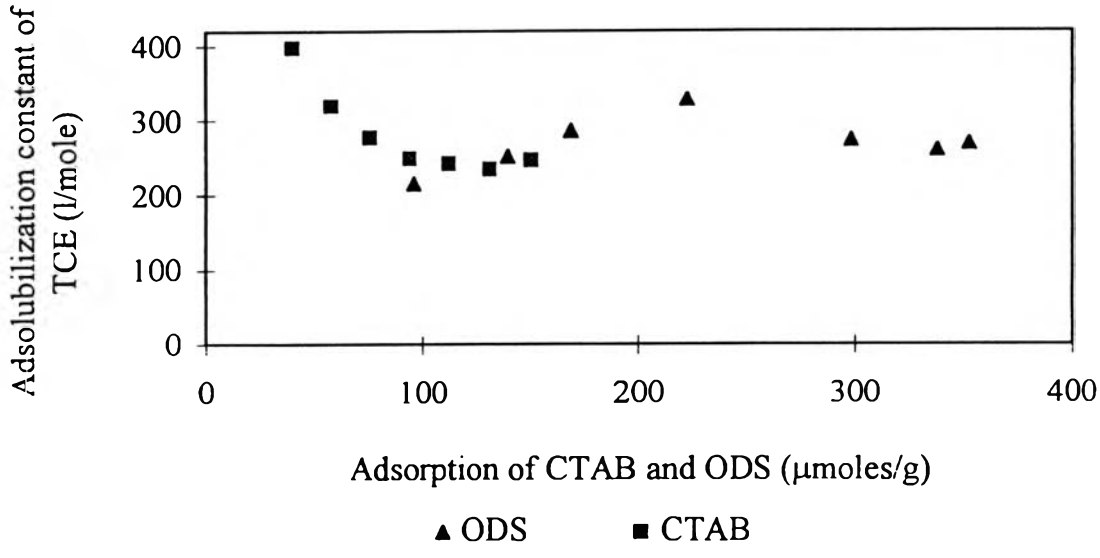

Figure 4.10 Effect of adsorption of CTAB and ODS on adsolubilization constant of TCE.

4.4 Stability of Bonded ODS Monolayer

The stability of ODS on silica was studied under various conditions. ODS loss was measured by the weight loss from TG-DTA and compared to that of initial value. Figure 4.11 shows the effect of agitation speed on desorption of ODS from silica. At rpm below 310, no ODS is observed in the bulk phase. Above this speed, ODS loss is found. The effect of agitation time is presented in Figure 4.12. No ODS desorption at agitation time of 60 min. ODS starts to desorb at 120 min. and has been found a little of 2.6 % loss at 180 min. Figure 4.13 shows the effect of pH on desorption of CTAB and ODS from silica. As can be seen in the figure, no loss of ODS was measured at various pH values with agitation speed of 210 rpm. Although the agitation speed is increased to 360 rpm, the ODS loss is not measurable when

pH is higher than 8. The lowest pH used, the ODS desorption is less than 2.0 %. Thus, contrary to physically adsorbed ionic surfactants, change in the surface charge affects the bonded ODS negligibly. The effect of temperature is reported in Figure 15. At temperature below 35 °C, no ODS loss was measured, but about 3.6 % loss was observed after 30 min. at 55 °C.

The stability of ODS under ozone condition is presented in Figure 4.15 and 4.16. Figure 4.15 indicates the relation between normalized remaining amount of carbon on silica surface (Co and Cm is the initial and final amounts of carbon) and oxidation time at various ozone concentrations. As the figure shows, it is encountered the very slow oxidation rate of ODS on silica surface. To compare with the oxidation of phenols (Gurol and Vastistas,

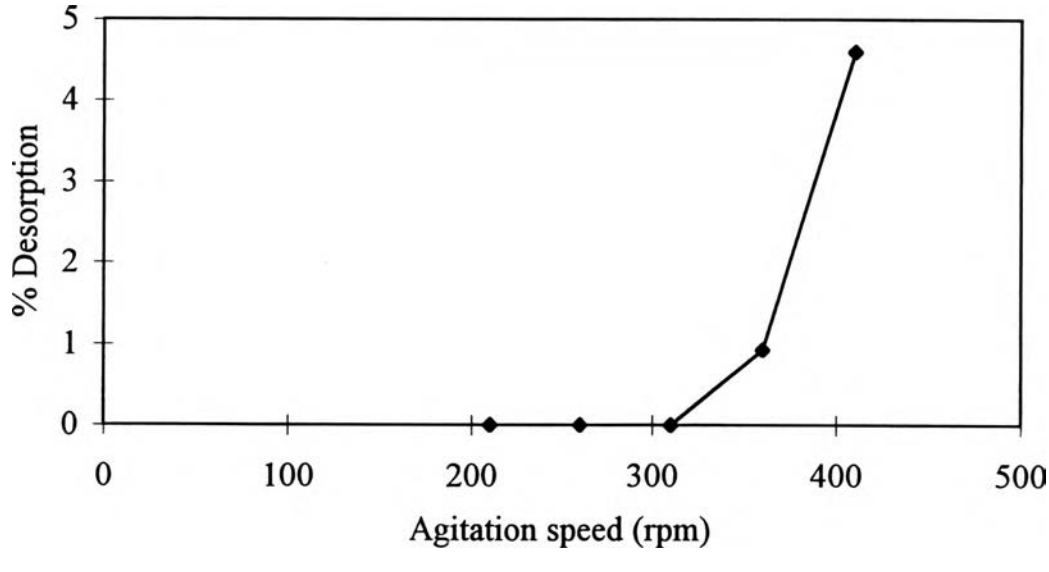

Figure 4.11 Effect of agitation speed on desorption of ODS from silica (30 min., pH 7 and 25 °C).

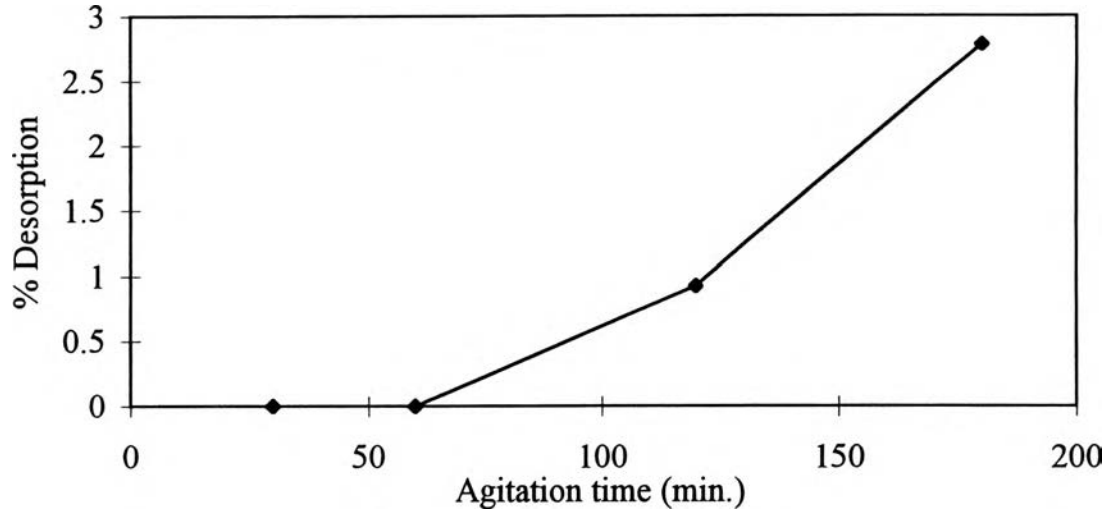

Figure 4.12 Effect of agitation time on desorption of ODS from silica (210 rpm, pH 7 and 25 °C).

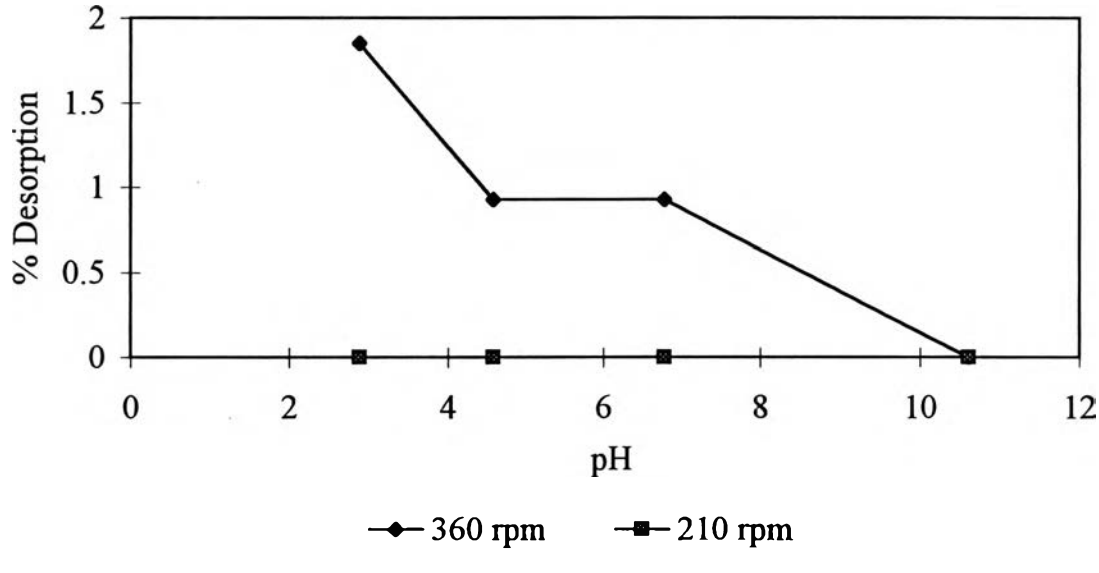

Figure 4.13 Effect of pH on desorption of ODS from silica (30 min. and 25 °C).

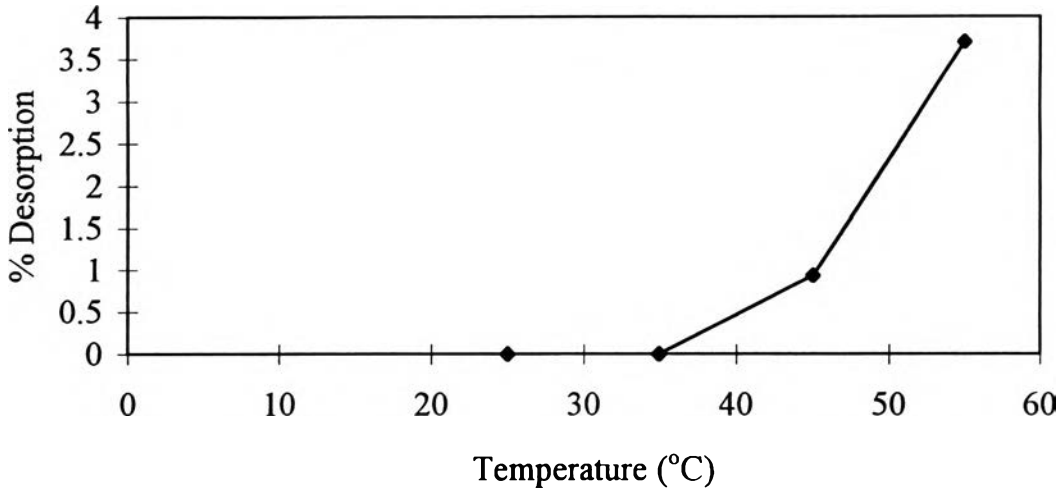

Figure 4.14 Effect of temperature on desorption of ODS from silica (210 rpm, pH 7 and 30 min.).

1987) and mecoprop (Beltran et al., 1994) by ozone, the very fast rate of oxidation is found within the first 20 min. Figure 4.16 shows the effect of pH on the oxidation of ODS on silica surface by ozone. It has been believed that ozone oxidation occurs by different mechanisms depending on the pH value (Hogine and Badder, 1976). Below the critical pH value of 7, ozone acts as an electrophilic oxidant, but at high pH the hydroxyl radical serves as the main oxidant. As be shown in Figure 4.16, the oxidation of ODS on silica surface by ozone is not affected at any pH values. Therefore, each type of oxidants shows an insignificant effect on the oxidation of ODS on silica. Thus, these results are useful for the oxidation of organic substrates by ozone because these substrates are oxidized very fast at high pH (Gurol and Vastistas, 1987) and in this study, ODS silica has a sufficient resistance to the oxidation of ozone at high pH value.

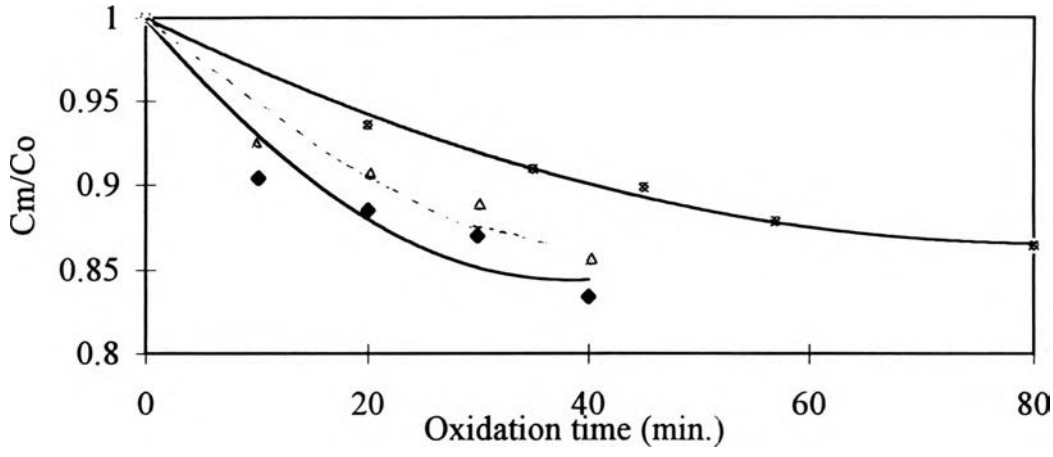

Figure 4.15 Stability of ODS silica at various ozone concentrations (pH 7 and 25 °C).

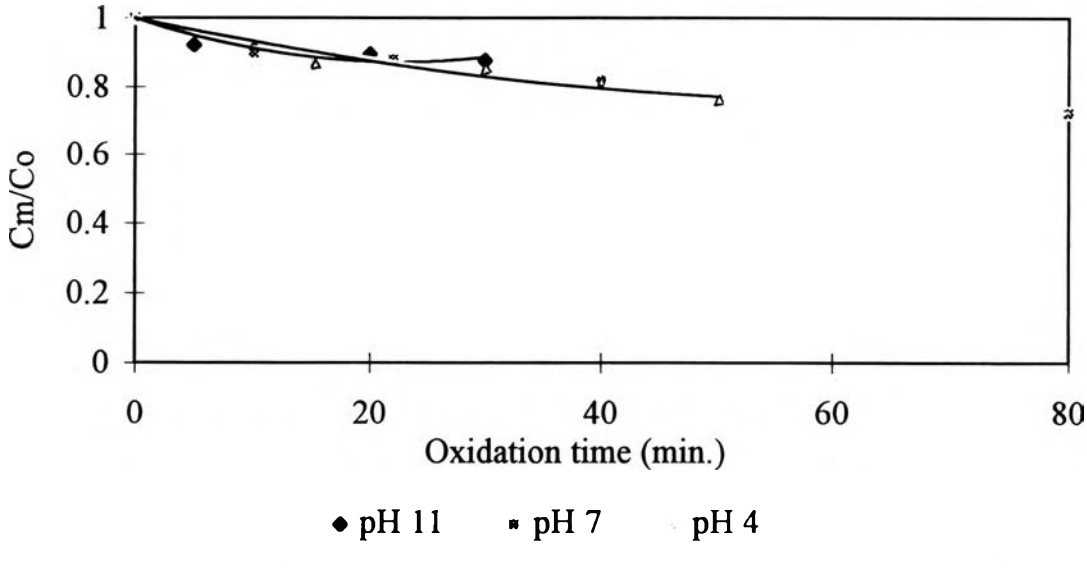

Figure 4.16 Stability of ODS silica under ozone concentration of 150 g/cm^3 at various pH values (25 °C).